

# Development of a Custom Made Condenser for a Two-Phase Thermosyphon CPU Cooling System

João Miguel Martins Lameiras  
joao.lameiras@tecnico.ulisboa.pt

Instituto Superior Técnico, Universidade de Lisboa, Portugal

November 2018

## Abstract

The present work aims at the development and characterization a custom air-cooled condenser to be implemented on a thermosyphon cooling system based on pool boiling and condensation of a dielectric fluid - HFE-7000. This gravity-assisted cooler is designed to be applied on a commercially available desktop CPU, to be capable of dissipating heat loads up to 250W. A numerical simulation was performed to define the design of the condenser, its main characteristics, dimensions and set of the most relevant geometric and working parameters. In line with this, the numerical simulation further addresses a parametric sensible study on the fin geometry of the condenser, to infer on the fin characteristics leading to the best performance in terms of heat transfer and fluid dynamics. The air-side heat transfer performance was evaluated based on the Colburn factor ( $j$ ) and the Fanning friction factor ( $f$ ) was determined to analyze the pressure drops. An experimental study was also performed on a viable benchmark, examining the condenser effectiveness and its effect on the overall cooling system thermal resistance. A multi-louvered fin heat exchanger with core's size of 110x120x22mm, which was the outcome of the numerical study, was manufactured and tested in the experimental study. The condenser was characterized both in reflux and circulation, under steady-state and transient regimes. In this experimental characterization of the condenser, other parameters such as the tilt angle, effect of microstructuring the surface on the evaporator and the effect of surface orientation were also addressed to evaluate their impact in the overall performance of the cooling system, incorporating the designed new condenser.

**Keywords:** Louvered fins, condensation, thermosyphon cooling, loop thermosyphon

## Acronyms

CLTPT	Closed Loop Two-Phase Thermosyphon
CPU	Central Processing Unit
CTPT	Closed Two-Phase Thermosyphon
HTC	Heat transfer coefficient
PFHE	Plate Fin Heat Exchanger
$A_o$	Total air-side surface area [mm <sup>2</sup> ]
$A_f$	Frontal area of the heat exchanger [mm <sup>2</sup> ]
$f$	Fanning friction factor [-]
$h$	Heat transfer coefficient [W/m <sup>2</sup> .K]
$j$	Colburn factor [-]
$p$	Pressure [mbar]
$q$	Heat rate [W]
$q''$	Heat flux [W/cm <sup>2</sup> ]
$R$	Absolute thermal resistance [K/W]
$T$	Temperature [°C]
$\epsilon$	Effectiveness [-]
$\delta_f$	Fin thickness [mm]
$\eta_f$	Fin efficiency [-]
$\eta_o$	Extended surface efficiency [-]
a	air-side
cond	condenser
evap	evaporator
j	junction
o	overall

sat	saturation
sys	system
w	wall

## 1. Introduction

The continued scaling of Internal Circuit technology together with the resultant ever-increasing power density and operating temperature poses significant challenges to engineers worldwide. Under high operating temperatures (above 80°C) the microelectronics performance is truly affected, having significant negative impacts on performance, power consumption and reliability [1, 2]. Hence, the junction temperature has become a major concern for high performance microprocessors, as more devices are integrated on a chip.

In order to solve the Thermal Power Management issue and keep with the improvement of microprocessors' performance, effective cooling techniques should be developed to dissipate the

increasingly large amount of heat from successively smaller areas. In this context, the technology of electronics cooling has become a key factor for further improvement of the performance of various electronic devices, especially microprocessors. Looking for higher dissipation heat fluxes, cooling with nucleate boiling is promising, as it removes dissipated heat within a wide range of fluxes and at relatively small surface temperature superheat. This technology benefits from the phase change latent heat of vaporization, being addressed as two-phase cooling technology.

### 1.1. Two-Phase Thermosyphon

The two-phase closed thermosyphon cooling is a gravity-assisted system composed by an evaporator, a condenser and connecting pipes. In the evaporator the microprocessor heat is absorbed into the system due to the nucleate boiling mechanism, while at the condenser the heat is dissipated to the ambient due to the condensation of the working fluid. A fan promotes the air force heat transfer convection in the condenser. The high heat loads which can be dissipated at low superheat temperatures, may lead to high heat transfer rates of condensation and boiling. The vapour generated at the evaporator rises due to buoyancy heading to the condenser. The condensate, in turn, returns into the evaporator due to a favorable gravitational head. Though this technology has been widely studied in the past for several high power dissipation applications, only recently attention was given to the application of this technique to microelectronics cooling. Hence, in the context of CPU cooling, fewer studies were conducted [3, 4] although its applicability has been proven effective and reliable. Beyond that, the existent two-phase thermosyphons studies are only focused on the evaporator and boiling heat transfer as well as on the overall system efficiency, being the work on evaluating the condensation and the condenser impact scarcely reported. It is known that the heat transfer processes in this kind of devices are significantly affected by the geometry, the inclination angle, the vapor temperature, operating pressure, the filling ratio and the thermophysical properties of the working fluid [5]. In most of the cases, the input working fluid is overfilled so that the liquid pool remains during the thermosyphon operation. However, excessive liquid charge is not appropriate. On the other hand, when there is not sufficient amount of working fluid to assure a stable operation of the device for a given heat input - underfilled case may lead to burnout [6]. The most significant criterion to evaluate thermosyphon performance is the thermal resistance [7].

A two-phase thermosyphon may be designed

as a single pipe CTPT or as a loop CLTPT. In the first case, the liquid and vapor flow in opposite directions (counter-current), also known as reflux. Under high heat fluxes, the interaction between these counter-current liquid and vapor flow and the viscous shear forces occurring at the liquid/vapor interface may inhibit the return of liquid to the evaporator (entrainment effect [8]). This results in a decrease in the amount of liquid returning to the evaporator and its eventual, while the liquid droplets are held in the condenser which becomes flooded [9]. If the evaporator section is not wet by returning fluid, the wall temperature significantly increases and the thermosyphon and/or the CPU may be permanently damaged. Furthermore, this two-phase flow in reflux mode introduces significant pressure fluctuations [10] which vary the saturation temperature and trigger temperature fluctuations. These instabilities may cause problems in maintaining steady and safe operating conditions at phase-change heat transfer devices. These operating limits are overcome in a loop, CLTPT, where the liquid and vapor flows are separated and the flow is unidirectional. So, a CLTPT generally depicts higher heat transfer coefficients than a CTPT. A conventional CLTPT is composed of an evaporator, a condenser and two connecting tubes - a rising (two-phase mixture from evaporator to the condenser) and a falling tube (condensed liquid back into the evaporator). In a CLTPT, the phase change processes take place at different temperatures in the evaporator and condenser. The saturation pressure in the evaporator is generally higher than that in the condenser counterpart. This differential saturation pressure assists to drive the coolant circulation within the loop. To ensure the required circulation rate to fulfill the cooling duty at the prescribed source-to-sink temperature difference for a CLTPT, the net driving pressure head is required to counteract the friction and form drags as well as the pressure drops attributed from flow acceleration/deceleration, bends, contractions and enlargements through the flow pathway. Note that the saturation temperature varies with pressure, which in turn affects the temperature differences for heat transfer. The heat transfer performance of the system is interdependent from its pressure drop.

Since the counter-current flow limitation seems to be a performance limitation at high heat fluxes, the use of thermosyphon loops with extended condenser surfaces has been suggested. In this study both arrangements are considered, namely the CLTPT with a single-pass condenser in circulation mode and the CTPT with counter-current flow, using the condenser in reflux mode. In line with this, the present work aims to develop and test a custom air-cooled condenser to be implemented on close

two-phase thermosyphon. This cooler is designed to be included in a commercially available desktop CPU and should be able to dissipate heat loads up to 250W.

## 1.2. Compact Heat Exchangers

Plate Fin Heat Exchangers (PFHE) are recognized as one of the most efficient, standard, and compact type of heat transfer devices. Hence, a PFHE was considered to be designed in this case study. High efficiency, small size, light weight and low cost are the desirable and relevant criteria in the fabrication of these types of compact heat exchangers. Heat transfer and hydrodynamic processes of the PFHE are strongly influenced by the configuration and geometrical parameters of extended surfaces. Plate fins are categorized as (1) plain, such as plain triangular and rectangular fins), (2) plain but wavy fins, and (3) interrupted fins, such as offset strip, louver, perforated, and pin fins.

In this work, a compact cross-flow PFHE was considered as air-cooled condenser. Corrugated multi-louver fins were used on the external air-side, forming the individual air-flow passages, while the flat tubes are responsible for the two fluid streams separation (air and coolant), as illustrated in figure 1.

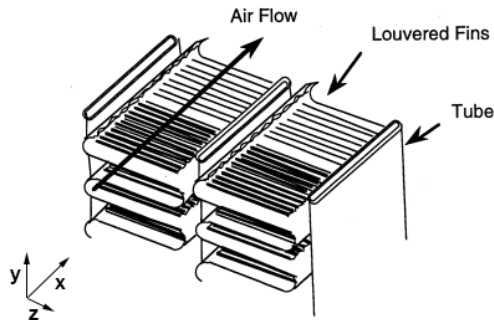


**Figure 1:** Schematic draw of a corrugated multi-louver fin and flat tubes.

The compact heat exchanger selected in the present work - a corrugated multi-louver fin and flat tube heat exchanger is widely used for systems, where high efficiency, low cost, small volume and light weight are vital requirements to fulfill. The main concept of the louvers is interrupt the air-flow and create a series of thin boundary layers that have lower thermal resistance and consequently higher heat fluxes. Besides that, the finned structure increases the surface contact area due to high level of compactness, resulting in heat transfer improvements. This configuration also provides lower drop pressures, when compared with conventional round tubes, due to smaller projected frontal area (flat tubes) causing less profile drag.

To understand if this type of finned plate heat exchanger would be efficiently applied as condenser

into this two-phase system, and if the air-flow speed (imposed by the fan's RPM) was enough to effectively improve the heat transfer processes, a numerical CFD simulation was performed.

## 2. Numerical Simulation - Condenser Design and Sizing

### 2.1. Computational Domain

A rectangular Cartesian coordinates system was used, with  $x$  representing streamwise direction,  $y$  wall normal direction and  $z$  spanwise direction. The periodic geometry along the flat tube,  $y$  direction and the symmetry along the air flow direction  $x$ , allow for simplification of the model geometry. A 3D model was divided into three main domains: the air flow domain, the flat tube domain and the fin domain. To fulfill the boundary conditions, the fluid

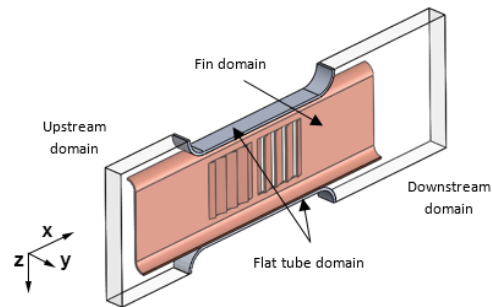


**Figure 2:** 3D computational domain.

domain was extended at the inlet (upstream), to allow a uniform air flow and especially at the outlet (downstream), in order to have a developed flow in the streamwise direction.

### 2.2. Governing Equations

A steady-state laminar flow analysis was performed considering the fact that flow has been proven to be laminar in the compact heat exchangers up to Reynolds number based on the louver pitch ( $Re_{Lp}$ ) of 1200 [11]. The flow is considered to be incompressible, since the air velocity is much lower than the speed of sound. The mass, momentum and energy conservation equations used in the analysis are shown in equations 1, 2, 3 respectively as follows:

$$\nabla \cdot \vec{u} = 0 \quad (1)$$

$$\vec{u} \cdot \nabla \vec{u} = -\frac{\nabla p}{\rho} + \nu \nabla^2 \vec{u} \quad (2)$$

$$\rho c_p \vec{u} \cdot \nabla T = \nabla \cdot (k \nabla T) + Q \quad (3)$$

The temperature distribution inside the solid regions of the model, such as the tube walls and fin, was obtained by solving the Fourier's law.

### 2.3. Boundary conditions

The boundary conditions used for the present domain are detailed below, where  $\perp$  and  $\parallel$  means perpendicular and parallel to the surface.

- Inlet face:  $\vec{u}_{\perp} = u_{in}$ ,  $\vec{u}_{\parallel} = 0$ ,  $T = T_{\infty}$ ;
- Outlet face:  $p = p_{atm}$ ,  $\frac{\partial T}{\partial n} = 0$ ;
- $x$ - $y$  faces of the fluid domain (lateral):  $\frac{\partial \vec{u}_{\parallel}}{\partial n} = 0$ ,  $\vec{u}_{\perp} = 0$ ,  $\frac{\partial T}{\partial n} = 0$  (symmetric B.C.);
- $x$ - $z$  faces of the fluid domain (bottom and top):  $\vec{u}_{bot} = \vec{u}_{top}$ ,  $p_{bot} = p_{top}$ ,  $T_{bot} = T_{top}$  (periodic);
- Fluid-solid interface:  $\vec{u} = 0$  (no slip);
- Inner flat tubes surface:  $q'' = h(T_{sat} - T_w)$  (convective).

Figure 3 depicts exactly which faces were detailed and their respective boundary condition.

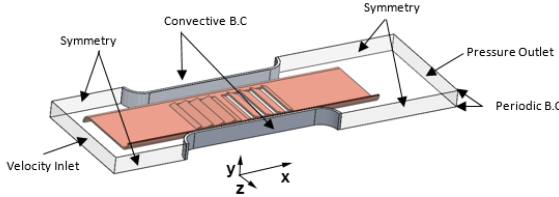


Figure 3: Boundary conditions of the computational domain.

A conjugate heat transfer 3D model was computed in COMSOL Multiphysics<sup>®</sup> v5.2, coupling the conduction of heat through solids with convective heat transfer in fluids.

### 2.4. Parametric Analysis to Improve Condenser's Performance

A sensitivity analysis evaluated the effect of several parameters, including fin pitch  $F_p$ , louver pitch  $L_p$ , louver angle  $L_{\alpha}$ , louver length  $L_l$ , redirection length  $S_2$  and louver number  $N_l$ . In figure 4 is shown the plain view and section cut of the study 3D model, evidencing all the parameters that influence the performance of the finned heat exchanger which are analyzed in this numerical study.

Within this scope, these geometric parameters were varied once at a time to obtain the best heat transfer performance possible, which was evaluated based on the Colburn and Fanning factors, as well as on the goodness factor which infers a valuable thermal-hydraulic performance quantification. This is still a basic analysis, only valid for  $Re_{L_p} = 20$ –250 corresponding to the maximum air-flow speed of 3m/s.

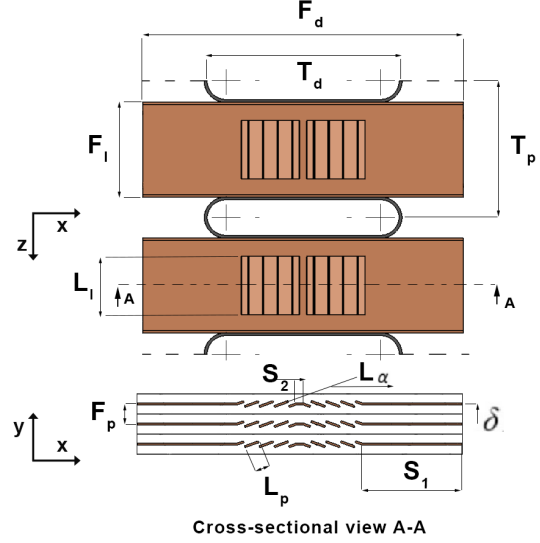


Figure 4: Definitions of geometric parameters for a multi-louvered fin and flat tube heat exchanger.

## 3. Data Reduction and Experimental Setup

### 3.1. Data Reduction

#### Thermal Circuit

The overall thermal resistance of the heat exchanger is considered to be composed by three components in series: (1) air-side thermal resistance  $R_a$ , including the extended surface efficiency, (2) wall thermal resistance  $R_w$  and (3) condensation thermal resistance  $R_i$ . Here the subscripts a and i denote the tube air-side and inside (coolant side) respectively. No fouling or scale resistance is considered on either side, so the corresponding resistance is not included in the calculations.

$$\frac{1}{U_o} = \frac{A_a}{A_i h_i} + \frac{A_a \delta_w}{A_w k_w} + \frac{1}{\eta_{o,a} h_a} \quad (4)$$

The wall thermal resistance is constant and the condensation heat transfer coefficients should be known a priori in order to calculate the overall thermal resistance. The term  $\eta_{o,a}$  in equation 4 is extended surface efficiency of the air-side surface and is related to the fin efficiency of the extended surface as follows:

$$\eta_{o,a} = 1 - \frac{A_f}{A_o} (1 - \eta_f) \quad (5)$$

$$\eta_f = \frac{\tanh(ml)}{ml}, \quad l = \frac{F_d}{2} - \delta_f \quad (6)$$

#### Effectiveness-Number of Transfer Units

The effectiveness-NTU method is used to evaluate the condenser effectiveness and to determine

the overall heat transfer coefficient used to validate the numerical results.

The heat exchanger effectiveness  $\epsilon$  can be shown that in general it is dependent on the number of transfer units NTU, on the heat capacity rate ratio  $C^*$  and the flow arrangement for a heat exchanger:

$$\epsilon = \phi(NTU, C^*, \text{flow arrangement}) \quad (7)$$

$$\epsilon = \frac{q}{q_{max}}, \quad C^* = \frac{C_{min}}{C_{max}} = \frac{(\dot{m}c_p)_{min}}{(\dot{m}c_p)_{max}} \quad (8)$$

$$NTU = \frac{1}{C_{min}} \int_A U dA \quad (9)$$

NTU, number of transfer units, designates the nondimensional heat transfer size or thermal size of the heat exchanger and therefore it is a design parameter.

For the specific case of the condenser  $C^* = 0$ , so the exchanger effectiveness expression 7 reduces to 10, valid for all flow arrangements.

$$\epsilon = 1 - \exp(-NTU) \quad (10)$$

### Thermal-Hydraulic Evaluation

The heat transfer and pressure drop characteristics were evaluated in terms of Colburn  $j$  factor and Fanning  $f$  factor [12] as a function of the Reynolds number based on louver pitch  $Re_{L_p}$ , calculated from:

$$Re_{L_p} = \frac{\rho u_c L_p}{\mu} \quad (11)$$

$$j = \frac{Nu}{Re_{L_p} Pr^{1/3}} = St.Pr^{2/3} \quad (12)$$

$$f = \frac{2\Delta p}{\rho u_c^2} \frac{A_c}{A_f} \quad (13)$$

where  $L_p$  is louver pitch,  $u_c$  is the critical air velocity at the minimum free flow area,  $\rho$  and  $\mu$  are the air density and dynamic viscosity respectively. In equation 13,  $\Delta p$  is the pressure drop and  $A_f, A_c$  are the frontal air-side surface area and minimum free flow cross area respectively. The results were also evaluated using the volume goodness factor  $j/f^{1/3}$  [13].

### 3.2. Experimental Setup

A custom heating device developed by Moura and Abreu [14, 15] was built to replicate the thermal behaviour of a real CPU, both in steady-state and transient conditions. The evaporator is an acrylic tube with 32mm inner diameter, 40mm height and 4mm thick. The evaporator section is electrically heated by a IRFP450 transistor with a contact area of 300mm<sup>2</sup> which is connected to a 60V power

source and controlled by the CPU and an electric board. This heating element is insulated by a teflon base. The condenser is assembled above the evaporator and mounted on a pivot joint with locking clamping lever support that enables to set the desirable inclination angle. The condenser's inclination angles are measured from the horizontal plane, where 0° corresponds to the horizontal position, positive values to upward and negative angles to downward flow.

Two condensers with multi-louver fins and flat tubes were experimentally tested at different configurations, circulation and reflux, as illustrated in figure 5. Hence, a standard 120x120mm condenser was used in reflux mode and the custom made 110x120mm single-passe condenser was implemented in circulation (closed loop). Both cross-flow heat exchangers are constituted by copper on the fins and brass on the flat tubes. Ini-

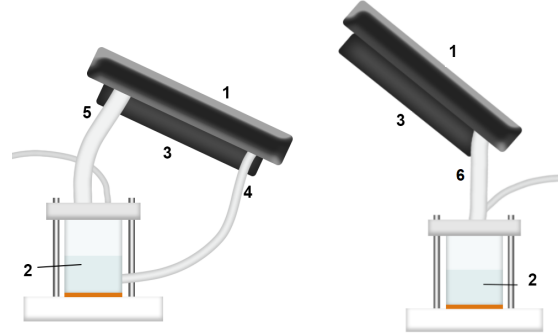


**Figure 5:** Horizontal experimental setup in circulation and reflux mode (left and right respectively). 1 - condenser; 2 - evaporator; 3 - fan; 4 - vapor line 5 - liquid line; 6 - two-phase line.

tially the condenser in circulation mode was positioned with a -30° tilt angle in order to enhance hydraulic drainage of the liquid film condensed, as suggested by Lip and Meyer [16, 17]. On the other hand, the condenser in reflux flow mode was positioned with a +40° tilt angle [18].

Seven K-type thermocouples manufactured by OMEGA were used to measure different sites. The junction temperature inside the transistor and the saturation temperature of the liquid in the evaporator are controlled variables and for this reason very important to acquire in this work. The ambient air temperature downstream and upstream to the condenser's fan forced convection air flow are also measured to infer on the condenser study.

### 3.3. Methodology

A manual working fluid degassing procedure is conducted at the beginning of each test. The experiments were performed under (1) steady-state and (2) transient conditions.

1. Steady-state experimental procedure consists on decreasing the dissipated power from the CHF, with small successive steps. Each experiment performed for a different imposed heat load was repeated five times. This study was performed under controlled pressure working conditions, via a PID controller implemented on LabVIEW. The evaporation pressure and consequently the boiling saturation temperature were controlled by the condenser's fan rotational speed.
2. Transient analysis procedure consisted on applying a cyclic heat load under Real Working Conditions. This means that the fan was set at constant RPM, with  $u_{air} = 3\text{m/s}$  measured by an anemometer to keep the air-flow speed. Temperature and pressure values are monitored for 140 seconds, being each test repeated three times.

## 4. Results & Discussion

### 4.1. Numerical Simulation

Numerical results have shown that the final optimized geometry enhances the air-side heat transfer coefficient when compared with corrugated plain fin heat exchanger for the same core's size and evaluated at the maximum air-flow speed ( $3\text{m/s}$ ). The HTC increases around 55%, which results in approximately 14.8% of heat flux enhancement. This results, in turn in a heat rate enhancement of 23.4% against the plain heat exchanger.

**Table 1:** Final thermal-hydraulic enhancement results compared with plain fin heat exchanger.

Model	Enhancement		
	$h(\%)$	$q''(\%)$	$j/f^{1/3}(\%)$
Manufacture	+22.8	+7.8	+8.8
Optimized	+55.0	+14.8	+18.9

However, due to manufacture restrictions, these optimized proposed dimensions were not possible to be applied in practice. Nevertheless, a local manufacturer - Construção de radiadores Lda. company, was able to manufacture and work on this type of louver fins after providing us their manufacturing limitations. So, an additional numerical simulation was performed to size and quantify the real gains of the condenser which could be actually manufactured and that was used in the following experimental activity, as detailed in the subsequent chapters. The final core's size of  $110 \times 120 \times 22\text{mm}$  was obtained with a TDP of  $250\text{W}$  (the maximum TDP value that is usually defined for modern CPU's). However, in a future work, providing that the current manufacture restrictions can

be overcome, the "optimum" geometry values obtained here will allow a reduction in the heat exchanger's transversal area of nearly 12% for the same heat dissipation of  $250\text{W}$ .

### 4.2. Experimental

With the increase of the heat load, the vaporization mass flow rate tends to increase, being unbalanced by the mass flow rate that is condensed. A way to improve condensation is therefore required to avoid this unbalancing. There are two alternatives, namely by spontaneously increasing the governing pressure within the closed loop - Real Work Conditions (RWC) - or forcing the raising of condensation rate by increasing fan RPM - Controlled Working Conditions (CWC). It is worth noting that along this work, the CWC was exclusively used for steady-state analysis. This condition was implemented for scientific purposes, in order to compare the experimental data obtained here with those reported in the literature, which are mostly obtained under controlled pressure conditions. The RWC was implemented only for transient-state analysis due to the implemented controller's insufficient response time to control the inner system pressure in a real CPU heat load demand.

The steady-state and unsteady-state experimental results discussed on the next paragraphs were obtained for  $30\text{ml}$  of HFE-7000 fill charge.

#### 4.2.1 Steady-State

##### Effect of Microstructuring the Evaporator Surface on System Overall Performance

The loop thermosyphon's overall thermal resistance (junction-to-ambient)  $R_{sys}$  is the sum of each component thermal resistance, more properly the solid heat conduction, the contact resistance and especially the boiling and condensation equivalent thermal resistances,  $R_{evap}$  and  $R_{cond}$  respectively.

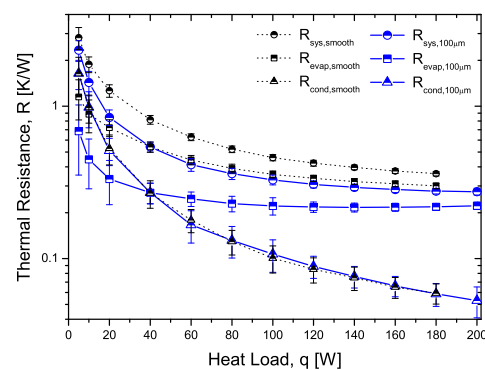


**Figure 6:** Thermosyphon loop's absolute thermal resistances under controlled pressure with different surfaces mounted on the evaporator: effect of surface microstructuring.



Figure 6 displays the relevant thermal resistance variables in a logarithmic scale, characterizing the thermosyphon loop performance with a smooth surface microstructured surface, composed by a regular pattern of microcavities with a fixed distance between them of  $S = 100\mu\text{m}$ . Detailed description of the procedures followed in the fabrication, preparation and characterization of this surface are reported in [14] and in [15].

The overall thermal resistance,  $R_{sys}$ , decreases significantly with increasing heat power. The lowest  $R_{sys}$  values were reached at maximum heat loads, namely  $0.361\text{K/W}$  for the smooth surface and  $0.276\text{K/W}$  for the microstructured surface. Microstructuring the surface enhances the boiling heat transfer in the evaporator, reducing the evaporator thermal resistance and consequently decreasing the overall resistance. Under maximum heat load demand, the junction temperature is nearly  $15^\circ\text{C}$  lower using the microstructured surface with  $S = 100\mu\text{m}$ , when compared to that obtained using the smooth surface. This temperature difference results in approximately 23% lower overall thermal resistance for the microstructured surface, when compared to that obtained with the smooth surface. This percentage tends to increase for lower heat rates, because the enhancement in the heat transfer coefficient obtained with the microstructured surface is larger for low heat fluxes, where the effect of bubbles coalescence, as described for instance by [19] is yet minimal. On the other hand, as expected, the condenser thermal resistance was not affected by the surface microstructuring in the evaporator.

### Effect of Condenser Orientation

Enhancing the condenser inner convective heat transfer coefficient leads to higher condensation rate that improves the cooler working operation. Besides that, lower temperatures and governing pressures are reached and consequently the junction temperature tends to be lower. The heat transfer coefficient - HTC inside tubes depends mainly on the mass flux and vapor quality. However, since it was not possible to determine precisely the mass flux or the vapor quality in the system, the condenser was characterized taking into account the heat load input. This experimental characterization was carried out for two types of condenser flows, namely (1) single-pass circulation and (2) reflux mode.

(1) Looking into the condenser in circulation mode, more precisely to the condensation inside tubes, the experimental mean condensation heat transfer coefficient was deduced from the Newton's Law of cooling. The effect of the condenser tilt angle was investigated in terms of HTC, for various

heat loads under steady-state as shown on figure 7.

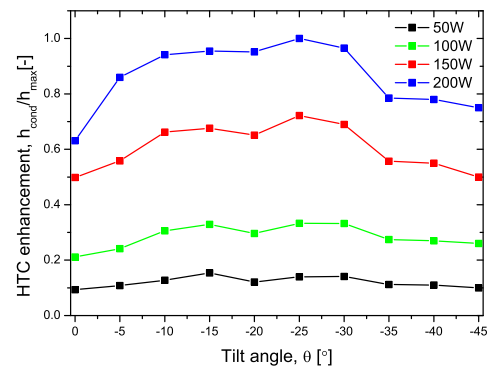


Figure 7: Tilt angle effect on HTC for different heat loads under controlled pressure conditions.

Concerning specifically the effect of the tilt angle, Lips and Meyer [17, 20], summarily refer that the effect of inclination is more pronounced at low mass fluxes, low vapour qualities and high saturation temperature. Depending on these parameters, [17] experimentally evidenced that there is an optimum inclination angle between  $-15^\circ\text{C}$  and  $-30^\circ\text{C}$  that leads to the highest heat transfer coefficient.

In this study, although lower mass fluxes are observed for low heat loads, the effect of inclination is more pronounced at higher heat loads. This result is not be entirely expected, looking at the aforementioned trends reported [17, 20]. Nonetheless, one should take into account that the mass fluxes in this system are lower when compared to those of Lips and Meyer. Furthermore, increasing the heat load, the mean vapor quality along the flat tubes of the condenser decreases due to the higher HTC, and the saturation temperature in the condenser slightly increases. Therefore, these results show that the optimum tilt angle for the system studied here is around  $-25^\circ$ . This was the tilt angle value that was implemented for the next experiments with this condenser in circulation mode. These conclusions are in agreement with most of the studies reported in the literature in this topic, suggesting that the impact of the tilt angle is not much sensitive to differences in the channel geometry.

(2) Reflux condensation refers to the condensation process that occurs in a vertical or an inclined tube in which vapor and liquid have a counter-current flow. The vapor flows upward driven by buoyancy forces, while liquid is flowing downward due to gravity. This gravity-controlled condensation process has been increasingly applied to compact plate heat exchangers, such as the case of the one

used in present work. This configuration would result in a more compact geometry, with lower liquid residence time and with less sub-cooling. Although larger sub-cooling is not considered an adverse effect, it should be avoided, since the sensitive heat transfer term is much lower, when compared to the that of the latent heat transfer. In this context, the system devised in the present work, accounted for the possibility of using a reflux condenser configuration. However, the operability of reflux condensers is limited by the phenomenon of flooding that appears at a critical vapor velocity at which the condensate starts to flow upward rather than downward. Flooding deteriorates the normal operation of the multiphase systems, which inevitably results in an abrupt increase of pressure drop. In the present configuration, it was concluded that the condenser inclination has low impact on the HTC enhancement under the reflux mode. For this reason, the selected angle,  $+40^\circ$ , was chosen taking into account the performed studies in this topic [18].

In summary, the condenser inclination angles used on the next experiments was  $25^\circ$  (downward) for circulation and  $40^\circ$  (upward) for reflux mode.

### Circulation vs Reflux

The effectiveness was determined for both condensers used in circulation and reflux mode, respectively and it was used to evaluate the condenser's performance. In this context, figure 8 depicts the heat exchanger performance along the applied heat load at steady-state.

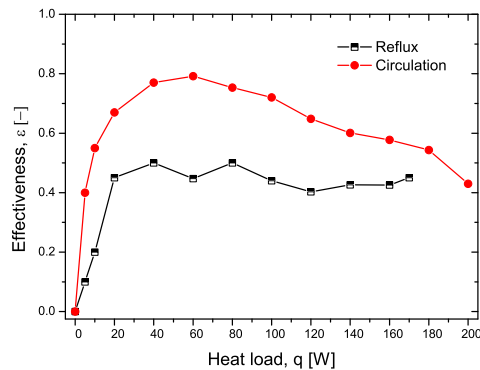


**Figure 8:** Condenser performance at steady-state - Reflux and Circulation.

The condenser's performance is also evaluated looking at the absolute thermal resistance (figure 9) for both reflux and single-pass flow configurations. Overall, the results support that the single-pass condenser in circulation mode has better effectiveness values and for this reason better performance results for all the applied heat load's range.

Furthermore, analyzing all the results one must conclude that despite all the potential advantages of using the reflux configuration, for the system devised here the condensation in circulation mode is preferred in steady-state working conditions as it overall shows better effectiveness for similar heat flux and thermal resistance, when compared to the reflux configuration.

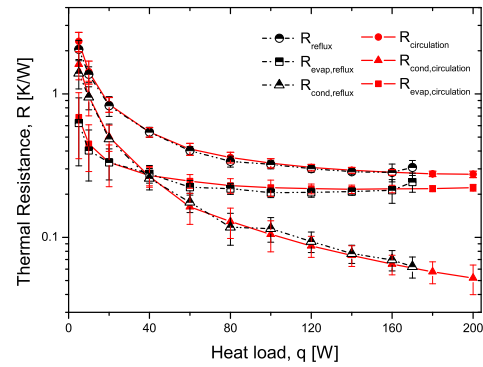


**Figure 9:** Thermal resistance for different condensers - Reflux and Circulation.

The overall thermal resistance for the maximum achievable dissipated power,  $q = 200\text{W}$  and  $q = 170\text{W}$  respectively, is  $R_{sys} = 0.275\text{K/W}$  for the circulation and  $R_{sys} = 0.303\text{K/W}$  with condenser in reflux mode. This means that in the closed loop thermosyphon at extreme power dissipation and stationary conditions the mean absolute thermal resistance is lower 7.5% than the reflux mode, resulting in a mean junction-air temperature decreasing of  $4^\circ\text{C}$  for  $170\text{W}$ .

### 4.2.2 Transient

In this sub-section the condenser's impact on the transient thermosyphon system is investigated under a cyclic load called here as I&M. Figure 10 allow taking useful conclusions to be used on the CPU cooling product development. The results, discussed in detail in the following paragraphs allowed concluding that the setup with condenser in circulation mode depicts quicker response time than that with reflux condensation, as shown on the plot by the steeper junction temperature response as well on pressure curves.

Despite the reflux mode's facility used 2 pipes instead of just one as in the circulation flow, an increase in the condensate mass flow was expected, which could cool down the working fluid temperature, decreasing the evaporator pressure and enhancing the overall cooler performance. However the pressure and temperature reduction are almost negligible as a minimal  $10\text{mbar}$  and  $0.5^\circ\text{C}$  decreasing of pressure and saturation temperature



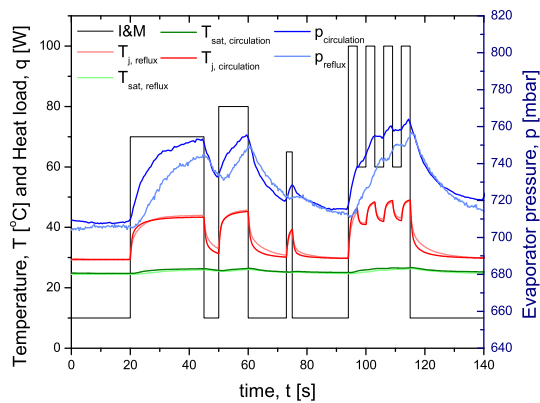


**Figure 10:** Thermal and pressure transient response for different condensers - Reflux and Circulation.

were observed, respectively. By the system response evolution previously discussed, it was possible to predict that the CLTPT system with condenser in circulation mode has better efficiency than CTPT with condenser in reflux mode. To confirm this prediction, an evaluation focused only on the condenser transient analysis was performed, where the instantaneous effectiveness values are depicted in figure 11.

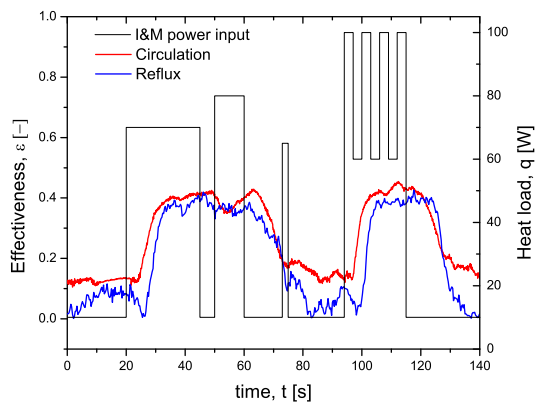


**Figure 11:** Condenser effectiveness at transient-state - Reflux and Circulation.

The condenser in reflux mode shows indeed lower effectiveness values than the circulation mode, which is in agreement with the analysis performed at steady-state. It is worth mentioning that the difference in the effectiveness in the circulation or in the reflux mode is much less prominent in the transient-state than in steady-state conditions. As also concluded in the steady-state study, it was also noticeable that in counter-current (reflux) flow condensation, the flow is much more unstable due to the vapor and liquid flow passage in the same tubes, promoting more fluctuations. This fact is

well visible in figure 11 by the condenser's effectiveness fluctuations, being also observed on the junction temperature, when the frequency is high enough (not in the presented graphics due to representation reasons). These conclusions are in agreement with many of the studies [10].

## 5. Conclusions

This study addresses the design and test of a condenser to be implemented in a thermosyphon cooling system, applied to commercial CPUs, which is able to dissipate up to 250W of heat power loads. This goal was achieved combining a numerical and an experimental approach. The first allowed to design and dimension the condenser, further allowing to perform a detailed analysis on the relevant parameters affecting the heat transfer and fluid dynamic processes in the condenser. The outcome of this analysis was a condenser with louvered fins and a core's size of 110x120x22mm, which was possible to build, under the current limitations pointed by the manufacturers. However, the analysis performed suggests that the condenser's transversal area could be reduced up to 12%.

The experimental approach addressed the test of the condenser in both circulation and reflux modes, in steady-state and in transient regimes. The study performed here allowed setting the following main conclusions, towards the development of a final functional cooling system:

- An optimum heat transfer was achieved with a condenser inclination of 25° downward for the circulation mode. The effect of the inclination angle was found negligible for the condenser working in the reflux mode.
- The condenser in circulation mode depicts better effectiveness than in the reflux mode (60% higher values than that of the condenser in the reflux mode). In the transient regime, the working mode of the condenser (circulation or reflux) has no impact on the working performance of the cooling system.
- The closed loop thermosyphon (circulation mode) achieves 18% higher CHF and lower 7.5% thermal resistance than the system with condenser in reflux mode. This results in a mean junction-air temperature reduction of 4°C for the same heat load of 170W.
- The closed loop two-phase thermosyphon with the condenser in circulation mode is more stable and leads to a better cooling performance of the entire cooling system.

Based on this analysis, the final closed loop thermosyphon system devised here achieved a  $R = 0.275\text{K/W}$  with  $q = 200\text{W}$  for horizontal orientation. These values were obtained using a microstructured surface with cavity distance of  $100\mu\text{m}$  in the evaporator, following the obtained in previous stages of development of the current system, which were confirmed in the present work.

## Acknowledgments

I would like to thank my supervisors Doctor Ana Moita for the scientific guidance and supervision through the course of this dissertation and Professor Doctor António Luis Nobre Moreira for having me in his laboratory team. Thanks also to Fundação para a Ciência e Tecnologia (FCT) for partially financing the research under the framework of the project JICAM/0003/2017, in the context of Projecto 3599 - Promover a Produção Científica, o Desenvolvimento Tecnológico e a Inovação.

## References

- [1] B. Sun and H. Liu, "Flow and heat transfer characteristics of nanofluids in a liquid-cooled CPU heat radiator," *Applied Thermal Engineering*, vol. 115, pp. 435–443, 2017.
- [2] K. Roy, S. Mukhopadhyay, and H. Mahmoodi-Meimand, "Leakage current mechanisms and leakage reduction techniques in deep-submicrometer CMOS circuits," *Proceedings of the IEEE*, vol. 91, no. 2, pp. 305–327, 2003.
- [3] T. E. Tsai, H. H. Wu, C. C. Chang, and S. L. Chen, "Two-phase closed thermosyphon vapor-chamber system for electronic cooling," *International Communications in Heat and Mass Transfer*, vol. 37, no. 5, pp. 484–489, 2010.
- [4] C. C. Chang, S. C. Kuo, M. T. Ke, and S. L. Chen, "Two-phase closed-loop thermosyphon for electronic cooling," *Experimental Heat Transfer*, vol. 23, no. 2, pp. 144–156, 2010.
- [5] Y. Kim, D. Hwan Shin, J. Sub Kim, S. M. You, and J. Lee, "Boiling and condensation heat transfer of inclined two-phase closed thermosyphon with various filling ratios," *Applied Thermal Engineering*, vol. 145, no. September, pp. 328–342, 2018.
- [6] H. Shabgard, B. Xiao, A. Faghri, R. Gupta, and W. Weissman, "Thermal characteristics of a closed thermosyphon under various filling conditions," *International Journal of Heat and Mass Transfer*, vol. 70, pp. 91–102, 2014.
- [7] R. Khodabandeh and B. Palm, "Influence of system pressure on the boiling heat transfer coefficient in a closed two-phase thermosyphon loop," *International Journal of Thermal Sciences*, vol. 41, no. 7, pp. 619–624, 2002.
- [8] J. Seo and J. Y. Lee, "Length effect on entrainment limitation of vertical wickless heat pipe," *International Journal of Heat and Mass Transfer*, vol. 101, pp. 373–378, 2016.
- [9] E. I. Drosos, S. V. Paras, and A. J. Karabelas, "Counter-current gas-liquid flow in a vertical narrow channel-Liquid film characteristics and flooding phenomena," *International Journal of Multiphase Flow*, vol. 32, no. 1, pp. 51–81, 2006.
- [10] G. Xia, W. Wang, L. Cheng, and D. Ma, "Visualization study on the instabilities of phase-change heat transfer in a flat two-phase closed thermosyphon," *Applied Thermal Engineering*, vol. 116, pp. 392–405, 2017.
- [11] A. A. Antoniou and T. A. C. M. R. Heikal, "Measurements of local velocity and turbulence levels in array of louvered plate fins," *Proceedings of the 9th International Heat Transfer Conference on Numerical Methods in Laminar and Turbulent Flow*, p. 482–495, 1987.
- [12] W. Kays and A. London, *Compact heat exchangers*. Krieger Pub. Co., 1984.
- [13] J. H. Kim, J. H. Yun, and C. S. Lee, "Heat-Transfer and Friction Characteristics for the Louver-Fin Heat Exchanger," *Journal of Thermophysics and Heat Transfer*, vol. 18, no. 1, pp. 58–64, 2004.
- [14] V. Abreu, "Test and optimization of a two-phase thermosyphon cooling system for microprocessors under real working conditions," Master's thesis, IST, Lisboa, Portugal, 2017.
- [15] M. Moura, "Design and development of a two-phase closed loop thermosyphon for CPU cooling," Master's thesis, IST, Lisboa, Portugal, 2015.
- [16] S. Lips and J. P. Meyer, "Two-phase flow in inclined tubes with specific reference to condensation: A review," *International Journal of Multiphase Flow*, vol. 37, no. 8, pp. 845 – 859, 2011.
- [17] S. Lips and J. P. Meyer, "Stratified flow model for convective condensation in an inclined tube," *International Journal of Heat and Fluid Flow*, vol. 36, pp. 83–91, 2012.
- [18] T. Klahm, H. Auracher, and F. Ziegler, "Heat transfer during reflux condensation of an R134a/R123 mixture in vertical and inclined narrow tubular and rectangular channels," *International Journal of Refrigeration*, vol. 33, no. 7, pp. 1319–1326, 2010.
- [19] E. Teodori, A. S. Moita, and A. L. Moreira, "Characterization of pool boiling mechanisms over micro-patterned surfaces using PIV," *International Journal of Heat and Mass Transfer*, vol. 66, pp. 261–270, 2013.
- [20] S. Lips and J. P. Meyer, "Experimental study of convective condensation in an inclined smooth tube. Part I: Inclination effect on flow pattern and heat transfer coefficient," *International Journal of Heat and Mass Transfer*, vol. 55, no. 1-3, pp. 395–404, 2012.